Eur. J. Mech. B - Fluids 19 (2000) 23–36

Low-speed streak and internal shear layer motions in a turbulent boundary layer

Marco Gottero, Michele Onorato *

Politecnico di Torino, Dipartimento di Ingegneria Aeronautica e Spaziale, Corso Duca degli Abruzzi 24, 10129 Torino, Italy

(Received 29 October 1998; revised 13 July 1999; accepted 23 July 1999)

Abstract – Some features of the inner region of a flat plate turbulent boundary layer are investigated by a Digital Particle Image Velocimetry technique. Measurements in planes parallel to the wall are examined. The energetic spanwise modes of the streaky motions are analysed by spatial Fourier analysis at different distances from the wall. Internal shear layers are deduced by applying VISA technique at $y^+ = 20$ and detected events are ensemble averaged. The deduced flow structure highlights the dominant spatial relationship between low-speed streak and internal shear layer motions. © 2000 Éditions scientifiques et médicales Elsevier SAS

Digital Particle Image Velocimetry / VISA technique

1. Introduction

After decades of experimental and numerical research, the structure of the inner layer of the turbulent boundary layers is still only partially understood. Large scale eddies were visualised by Reynolds in a pipe flow in late 1883. After this early work, the research activity was dominated by the statistical theory of turbulence for many decades, until the flow visualisation studies of Kline et al. [1], Corino and Brodkey [2] and Kim et al. [3]. These studies provided evidence that organised and deterministic motions are re-occurring features in the inner layer of wall turbulent flows and are responsible for most of the turbulence production. After these pioneering works, various non-random events have been experimentally identified, such as wall low-speed streaks, internal shear layers, vortical structures, ejections and sweeps.

An important part of the experimental investigation has dealt with detection methods of the organised motions and hence with their frequency of occurrence and with conditional averaging of the part of the velocity signal corresponding to the event (Blackwelder and Haritodinis [4]). An exhaustive review article of these researches may be found in the paper of Robinson [5].

Very few attempts have been made to determine the spatial and temporal relationships between the various experimentally detected structures. The reason is that one or a small number of fixed probes are not adequate to observe the characteristics of the three-dimensional turbulent organised motion with large variations in space and time.

After years of activity, until the evidence of results from direct numerical simulation, no substantial advances have been made experimentally from the scenario described by Kim et al. [3], using the hydrogen-bubble technique. They recognised that most of the turbulence production in the boundary layer occurs during a dynamic process termed ‘burst’. According to this process, the low speed streaks, after remaining stable for some streamwise distance, begin to oscillate and lift away from the wall, breaking down and giving rise to the

* Correspondence and reprints; onorato@polito.it

ejection of low speed fluid into the outer flow. Strong internal shear layers are then detected by a fixed probe when an ejection passes through the detection point, producing a rapid change in the instantaneous streamwise velocity component. It was also recognised during these experimental studies that elongated vortices or hairpin vortices play an important role in the formation of low speed streaks, although they appear to be one order of magnitude shorter than streaks in the wall region (Robinson [5]).

More recently, the development of simulation methods for turbulent flows (DNS) has introduced substantial changes in studying turbulence producing events. Even if limited to low Reynolds numbers and simple geometry, the databases generated from DNS allow a complete three-dimensional space–time mapping of all components of the velocity field. Nevertheless, the understanding of all the processes leading to the production of turbulence in the near wall region is not straightforward.

Guezennec et al. [6], analysing the Kim et al. [7] turbulent channel flow DNS database, at $Re_{u_\tau} = 180$, pointed out that instantaneous turbulence producing events are predominately associated with asymmetric vortical structures. They observed that sometimes a vortex is followed by another one of opposite sign rotation, forming a staggered array. In addition they found that these structures are convected downstream for a great distance with few changes, indicating that they do not enter into a catastrophic break-up process due to an instability mechanism. Johansson et al. [8], again from the analysis of Kim et al. database [7], observing the lack of a violent break-up stage following small-scale oscillatory motions of the structures, affirm the need to revise the conceptual models of the bursting process. They detected shear-layer structures in the buffer region using the VISA technique, a spatial counterpart to the VITA (Variable Interval Time Averaging) technique of Blackwelder and Kaplan [9]. It was found that strong instantaneous streamwise gradients (internal shear-layer structures) are generated in a process where neighbouring elongated high- and low-speed regions interact through a localised spanwise motion, producing a meandering of the streaky pattern. Bernard et al. [10], using a vortex identification scheme based directly on the vortex rotational motion, were able to locate the entire set of vortices in the near wall flow field ($y^+ < 100$) of a turbulent channel flow ($Re_{u_\tau} = 125$) simulation (Handler et al. [11]). The main objective of their research was to study the dynamic role of the vortices in producing Reynolds stress. They attribute the generation of ejection and sweep events to the mutual interactions of the quasi-streamwise vortices, convected at different velocities in the near wall region; as vortices of opposite streamwise rotation come closer, they form localised regions characterised by ejections or sweeps. Moreover, as in Brooke and Hanratty [12], quasi-streamwise vortices are found to originate close to the wall in response to the intense spanwise shearing by pre-existing analogous vortices. Chacin et al. [13], based on the argument that vorticity is a poor marker of vortical structures in a wall shear layer, identified structures with the use of the cubic discriminant related to the invariants of the velocity gradient tensor. Studying the Spalart [14] numerically simulated turbulent boundary layer over a flat plate ($Re_\theta = 670$), they showed that loci of constant positive discriminant ($D > 0$) consist of coherent elongated regions aligned with the main shear close to the wall and forming into an arch in the cross-stream direction away from the wall. These structures, in some cases, are reminiscent of the hairpin eddies proposed by Theodorsen [15]. They found that regions of high instantaneous values of Reynolds shear stress are situated at the edges ($D > 0$) of the structures. Jeong et al. [16] detected vortical structures in the DNS channel flow of Kim et al. [7], at $Re = U_c h/\nu = 3300$, connecting regions where the second largest eigenvalue of the tensor $S_{ik}S_{kj} + \Omega_{ik}\Omega_{kj}$ is negative (Jeong and Hussain [17] detection scheme); S_{ij} and Ω_{ij} are the symmetric and anti symmetric parts of the velocity gradient tensor. The primary objective of the paper was to study the spatial relations of near wall coherent structures with experimentally observed turbulence producing events in the buffer layer. They developed a conceptual model of coherent structures in the near wall region that summarises most of the recent findings, among others Johansson et al. [8], Robinson [18], Jimenez [19]. According to this model, the inner layer up to $y^+ = 60$ is dominated by quasi-streamwise elongated vortices, slightly inclined and tilted; the motion appears to be organised in sequences in which vortices of alternating signs overlap in the streamwise direction as a staggered array. No evidence of

hairpin vortices was observed in the near wall analysed region. Based on this model, nearly all experimentally observed events and their mutual relations appear to have a rational interpretation.

While the presence and prominence of quasi-streamwise vortices and low-speed streaks in the wall region is now generally accepted and their knowledge can be considered well founded, the evolutionary dynamics of such structures already need further clarification. Schoppa and Hussain [20], on the base of the Jeong et al. [16] conceptual model, recognise the streaky quasi-steady base flow to be the necessary and sufficient ingredient for the regeneration of new longitudinal vortical structures. They show that a non-linear instability of lifted low-speed streaks, free from any initial parent vortex, directly generates new streamwise vortices, which in turn induce and sustain the wall streaks. This regeneration cycle, in contrast with the mechanism based on the induction of secondary vorticity at wall, is confirmed by the numerical experiments of Jimenez and Pinelli [21]. The last authors, manipulating the wall flow by filtering the low-speed streaks without directly perturbing the vortices, show that the wall turbulent flow decays viscously to laminar flow.

Although the use of databases generated from direct numerical simulation have become a feasible alternative to the experimental investigation for low Reynolds number flows and simple geometry, experimental methods will continue to be the only realistic approach for wall turbulence studies of non-canonical situations at higher Reynolds numbers and complex boundary conditions. Moreover, the development of advanced instrumentation may contribute to the removal of existing inconsistencies arising from the interpretation of the enormous amount of information contained in numerical databases. Advanced experimental methods are becoming available to accomplish these tasks, most of them based on optical anemometry techniques.

A quantitative flow visualisation methodology, suitable for turbulence investigation, has been developed at the Laboratorio di Anemometria Ottica of the Centro di Studio per la Dinamica dei Fluidi del CNR. The objective is the application to complex flows, such as ‘manipulated’ boundary layers for drag and heat transfer control (Gottero and Onorato [22,23]).

In this paper results from the investigation of turbulent boundary layer over a flat plate will be shown. The flow in planes parallel to the wall, in the buffer layer and logarithmic regions, is analysed, highlighting the spatial relationship between low speed streaks and internal shear layers.

2. Experimental set-up and procedures

Experiments were carried out in the ‘Hydra’ water tunnel. This facility is a closed loop, open flow channel, with $350 \times 500 \times 1800$ mm test section. Measurements were taken on a flat plate positioned in the test chamber, with transition fixed at the leading edge. The observed section is characterised by $Re_x = 4 \cdot 10^5$, $Re_\theta = 1010$, $H = 1.41$, $C_f = 0.0042$, $u_\tau/u_e = 0.046$, $\delta = 35$ mm. A double-pulsed light sheet is provided by a Nd-YAG laser source (200 mJ and 8 ns per pulse). The flow is seeded with spherical solid particles, 2 μm nominal diameter. Seeding concentration, about 10^{-7}, is low enough to prevent alteration of flow properties and interaction between particles. A particle relaxation time τ and a buoyancy velocity v_g may be evaluated from

$$\tau = \frac{\rho_p D^2}{18\mu_f} \quad \text{and} \quad v_g = g\frac{(\rho_p - \rho_f)D^2}{18\mu_f},$$

where ρ_p is the density of the tracers, D their nominal diameter, ρ_f and μ_f the density and the viscosity of the fluid. It comes out that the particle relaxation time is 10^{-4} times the Kolmogorov time scale and the buoyancy velocity is $5.2 \cdot 10^{-3}$ mm/s, corresponding to a displacement of $6 \cdot 10^{-4}$ pixels, one order of magnitude smaller than the errors due to all other inaccuracy sources.

Images of the seeded flow in illuminated planes parallel to the wall are captured on a photographic high-resolution 24 × 36 mm film. Time statistics have been obtained from series of digital CCD video camera images, in planes normal to the wall and parallel to the mean flow. In this case the time resolution of the data is governed by the double-pulse repetition rate of the laser (12.5 Hz).

Analysis algorithms are based on a two-dimensional digital particle image velocimetry technique, DPIV (Adrian [24], Willert and Garib [25], Westerweel [26]). The capability of this technique to provide non-intrusive and accurate full-field measurement of the instant velocity field makes the technique particularly attractive in the spatial characterisation of turbulent flow structures.

Special accuracy and resolution are needed in analysing the details of turbulent flows (Kompenhans and Hocker [27], Eggels et al. [28], Westerweel et al. [29]). Procedures have been developed to match the requirements and preserve, at the same time, velocity and flexibility of analysis: dynamic control of acquisition and analysis parameters and minimisation of free parameters, minimisation of pre-processing before image interrogation, digital image-shifting algorithms (reduction of the sub-pixel interpolation error), full automatisation of the process, automatic procedures for data validation, etc. Moreover, in order to perform a parametric study of analysis accuracy, homogeneous and isotropic turbulent flow fields were simulated by random Fourier modes variable in time and space covering a limited range of wave numbers (Fung et al. [30]). The simulated velocity field is given by

$$\mathbf{v}(x_i, t) = \sum_{n_i=-N_k}^{N_k} \left[S_{n_i} \cos(k_{n_i} x_i + \omega_{n_i} t) + R_{n_i} \cos(k_{n_i} x_i + \omega_{n_i} t) \right] \quad (i = 1, 2)$$

(with $k_{n_i} = 2\pi n_i / X_i$; ω_{n_i}, S_{n_i} and R_{n_i} random coefficients).

Synthetic images representing the motion of solid particles were created from these simulated velocity fields and analysed. In this operation, the light diffracted by tracer particles is assumed to generate a Gaussian distribution of grey levels; the raster generation is substituted for the digitalisation. A certain loss of particles and fuzziness of images due to the out of plane velocity component is admitted; background random white noise is introduced. Series of the obtained images were analysed, systematically varying the main parameters: seeding concentration, tracer nominal diameter, mean velocity and turbulence intensity, out of plane motion. Results of these tests and of complementary experimental investigation show that measurement global error on absolute displacement is less than 0.15 pixel and low enough to allow turbulence measurements.

Space–time resolution of the analysis has been evaluated referring to Grotzbach criteria for numerical simulation (Grotzbach [31], Eggels et al. [28]). In particular, the measurement volume Δ^3 has been compared with the Kolmogorov length scale η and the measurement time interval Δt with the corresponding time-scale τ_k. For an effective thickness of the laser sheet of $\Delta z_e = 0.25$ mm and an interrogation linear window size of 1.6 mm (64 pixels), we obtain $\Delta = 0.83$ mm; estimating $\eta^+ = 1.5$ (Antonia et al. [32]), it follows that $\pi\eta = 0.35$ mm: the spatial criterion, $\Delta < \pi\eta$, is exceeded by a still acceptable percentage if compared with the whole range of scales. The time resolution requirement is widely satisfied: $\Delta t/\tau_k = 0.08$. Significant flow statistics and an appropriate evaluation of differential quantities down to very small scales, of the order of Taylor microscale, can be achieved.

The out-of-plane velocity component can be estimated by comparing the out-of-plane particle displacement, Δs_0, with the effective thickness of the laser sheet, Δz_e. Assuming $\Delta s_0 = u_\tau \times \Delta t$, it is found that $\Delta s_0/\Delta z_e = 7 \cdot 10^{-2}$; the out-of-plane 'loss of pairs' is small and the stereoscopic error of 2D PIV recording is negligible here.

3. Results and comments

3.1. Statistical and spectral analysis

To demonstrate the accuracy of the experimental technique and characterise the turbulent flow, a time statistic analysis has been carried out on a series of more than 500 video-camera images in a plane (x, y) normal to the wall, parallel to the mean flow and located at the centreline of the plate. Mean and fluctuating velocity profiles, not shown here, are in good agreement with data from the literature (Wei and Willmarth [33]).

The possibility of determining spatial distributions of the flow variables represents a fundamental step in the laboratory investigation of coherent motions. With the intention of analysing the spatial structure characterising the inner region of the turbulent boundary layer, a series of planes parallel to the wall at different distances y^+ have been investigated. Images from the photo-camera have been used in order to take advantage of the higher accuracy and resolution of the film, more than 5000 lines with a standard format of 24×36 mm. Results of frozen velocity fields in three planes (x, z) parallel to the wall, at a distance of 20, 70 and 130 wall units, will be shown here.

In *figure 1* a grey-level map and contour plot of the instantaneous longitudinal fluctuating velocity u, in a plane (x, z) at a distance from the plate of 20 wall viscous lengths, $y^+ = 20$, is shown. The observed flow field covers about 700 viscous units in the longitudinal direction and 1050 viscous units in the transverse direction.

As expected in the buffer-layer region, quasi-streamwise low speed streaks characterise the flow. The typical irregular wavy appearance of the streaky structures seen in theoretical models (Landahl [34]) as well as in the numerical simulations (Johansson et al. [8]) is also clearly evident in the present results. The importance of this meandering of the streaky patterns in producing steep streamwise and spanwise gradients of u will be shown later.

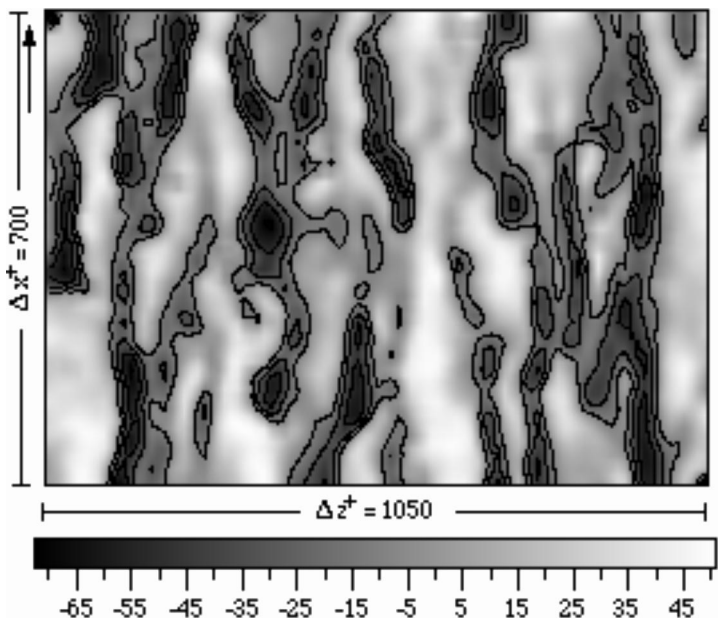

Figure 1. Grey-level map and iso-contour plot of the streamwise turbulent u-velocity component in mm/s; $y^+ = 20$. Contours $= -70, -10$ increment 20.

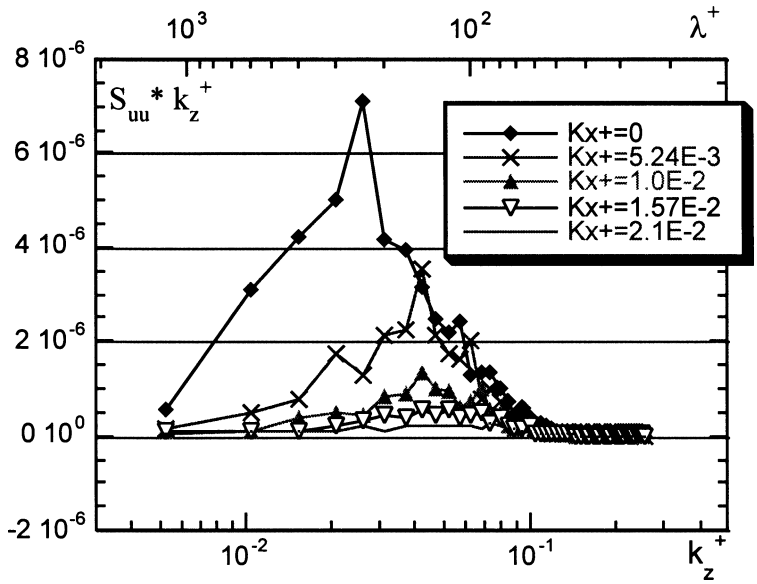

Figure 2. Two-dimensional Fourier spectrum of the streamwise velocity component; $y^+ = 20$.

The streamwise extent and spanwise spacing of the streaks have been the subjects of several investigations, both experimental and numerical. Several authors report estimations of streamwise scales varying from 500 to more than 1000 wall units, with widths ranging from 20 to 80 ν/u_τ. The reported mean spanwise spacing is about 100 viscous units, $\lambda^+ = 100$, in the viscous layer, increasing to a value of about $\lambda^+ = 140$ at the external edge of the buffer layer (Smith and Metzer [35]), essentially invariant with Reynolds number. Values of λ^+ have generally been obtained by visual inspection of flow visualisations or of numerically simulated data and are confirmed in the present DPIV images. An objective criterion for defining appropriate lengthscales is based on the evaluation of the energetic content of each scale by using spectral analysis. DPIV data allow quantitative evaluation of the spanwise modes of the streaky motions by two-dimensional Fourier analysis, as suggested by Liu et al. [36]. *Figure 2* displays the spatial Fourier spectrum versus spanwise wave numbers, k_z, with streamwise wave numbers, k_x, as parameters, obtained by averaging 15 time independent realisations similar to that in *figure 1*. S_{uu} is the two-dimensional power spectrum of the u-velocity component normalised with respect to the external flow velocity U_e^2: the power spectrum, S_{uu}, is multiplied by the spanwise wavenumber. The spectrum in *figure 2* reveals that the streaky structures have many spanwise modes and that the most observed mode by flow visualisation, $\lambda^+ = 100$, is relatively weak compared with modes related to larger scales. This is in agreement with results of Liu et al. [36] in a turbulent channel flow. The most energetic spanwise mode, here observed, occurs at $\lambda^+ = 2\pi/k_z^+ = 260$.

Figures 3 and *4* show maps of the instant longitudinal fluctuating velocity in planes (x, z) at a distance from the plate of 70 and 130 viscous lengths respectively. As already found (Smith and Metzer [35]), in the logarithmic layer the streak spanwise spacing increases and the streamwise scale decreases with the distance from the wall. At a larger distance from the wall the streak visual identification becomes very uncertain. Kline [37] suggests $y^+ = 40$ as the upper limit for which well-defined streaks can be identified. In *figure 5* power spectra are shown for the three planes, for $k_x^+ = 0$. This quantitatively confirms the increasing of the spanwise scales in the logarithmic region. The most energetic modes occur on scales of $\lambda^+ = 370$ and $\lambda^+ = 490$, for $y^+ = 70$ and $y^+ = 130$ respectively, as a consequence of the increase of the streak spanwise spacing.

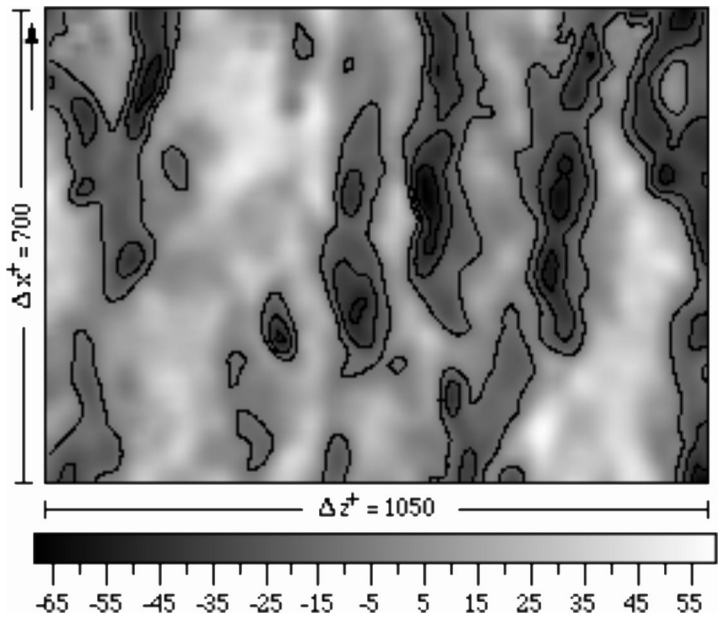

Figure 3. Grey-level map and iso-contour plot of the streamwise turbulent u-velocity component in mm/s; $y^+ = 70$. Contours $= -50,\ -10$ increment 20.

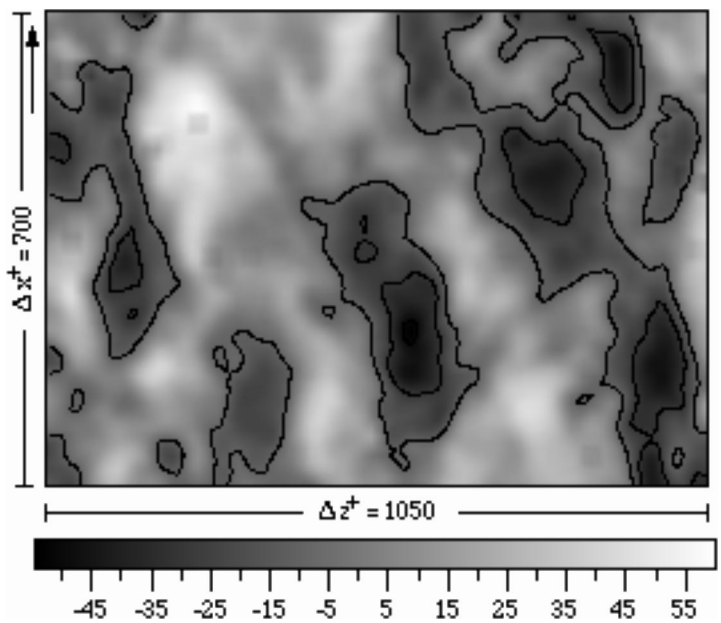

Figure 4. Grey-level map and iso-contour plot of the streamwise turbulent u-velocity component in mm/s; $y^+ = 130$. Contours $= -50,\ -10$ increment 20.

The black spots in *figure 6* indicate VISA (Variable Interval Space Average) events, namely regions where the locally averaged u-variance exceeds the mean variance; a contour plot of the instant u-velocity is also reported. *Figure 6* refers to the same instant and position ($y^+ = 20$) of *figure 1*. The VISA technique is the spatial counterpart of VITA (Variable Interval Time Average) technique (Blackwelder and Kaplan [9]), extensively

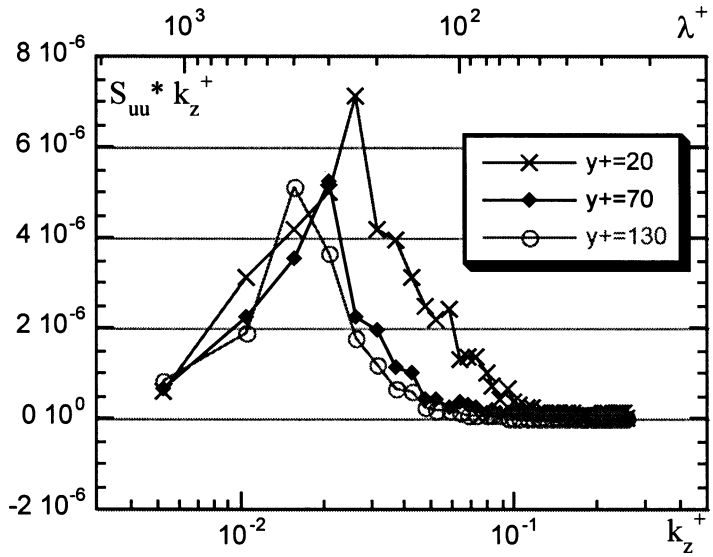

Figure 5. Fourier spectra of the streamwise velocity component at different distances from the wall; $k_x^+ = 0$.

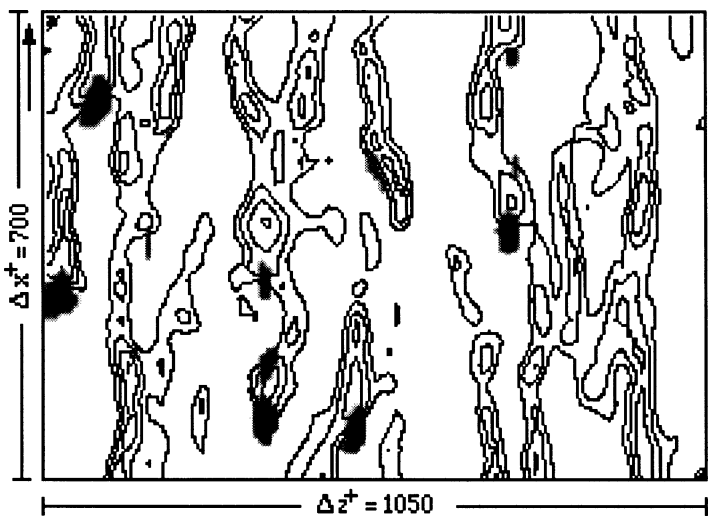

Figure 6. Location of VISA events (black spots) in the instant u-velocity field of *figure 1* (contour lines).

used to detect internal shear layer motions. The local variance was averaged over a 'short integration distance' in the streamwise direction of 115 viscous units. This length, assuming a propagation velocity of the shear layers of 10.6 u_τ (corresponding to the local mean velocity and in agreement with Johansson et al. [8]), refers to a 'short averaging time' of 10 viscous units. This averaging time, $T^+ = 10$, has been used in most studies to detect VITA events from hot wire probe signals. In order to compare the present DPIV experiments with Eulerian probe measurements, the number of events per unit time has been deduced from 15 realisations as shown in *figure 6*. For this analysis a procedure similar to that of reference [8] was adopted. The average number of detections per z-position was determined and normalised by the streamwise extent of the domain divided by the propagation velocity. This procedure yields a result equivalent to the number of detections per unit time for a fixed probe. Also, the averaging length was converted to an equivalent averaging time by use of

the propagation velocity. A non-dimensional frequency $f^+ = f\nu/u_\tau^2$ of $3.2 \cdot 10^{-3}$ has been found, in agreement with hot wire literature.

Representations of the flow field as in *figure 6* are suitable for observing the spatial relationship between low speed streak and internal shear-layer motions. High levels of local variance are localised along the boundaries of the streaks; the strongest events, always with $\mathrm{d}u/\mathrm{d}x < 0$, are found by the side of the streaks, often near the upstream end of the region where the streak seems to divide or to change the tilting direction. The characteristics of the streaks of appearing as segmented elements alternately tilted with respect to the mean flow, seems to be essential in the production of strong internal shear layers.

3.2. Conditional analysis

A conditional analysis has been applied to a series of instantaneous images at $y^+ = 20$. Detected internal shear layer events were ensemble averaged centring individual realisations in both x and z directions. The VISA technique has been modified in order to retain asymmetry features of the streaks: individual events with different sign of $\mathrm{d}u/\mathrm{d}z$ have been ensemble averaged separately. Only accelerated events ($\mathrm{d}u/\mathrm{d}x < 0$) have been considered. In *figure 7* the results corresponding to $\mathrm{d}u/\mathrm{d}z < 0$ are shown; the VISA detection point, corresponding to the peak of the local u-variance, is at $x^+ = z^+ = 0$; continuous and dotted contour lines highlight phase averaged low-speed and high-speed bands respectively. The superimposed velocity vector field represents the conditionally-averaged fluctuating velocity parallel to the wall. Results corresponding to $\mathrm{d}u/\mathrm{d}x > 0$ are specular with respect to results in *figure 7*. The ensemble-averaged structures retain most of the characterising features of single realisations. In particular, the segmented character of the streaks is clearly shown in the iso-contour plot by the two low-speed islands tilted in different directions. The position of the internal shear layer event ($x^+ = 0,\ z^+ = 0$), highlighted by the distribution of $\mathrm{d}u/\mathrm{d}x$ in *figure 8*, corresponds to the merging region of the two kinked low-speed segments, at the border between low and high-speed bands. This characteristic asymmetric feature of the elongated segmented low-speed streaks seems of great importance for the generation of the internal shear layer structures; these are in turn to be considered the main contributor to the production of turbulence. The structures in *figure 7* bear a close resemblance to results obtained by Johansson et al. [8] by applying VISA technique to the turbulent channel flow DNS data of Kim et al. [7]; a similar picture is presented by Jeong et al. [16] as an outcome from the application of Jeong and Hussain [17] vortical structures detection scheme to the same data base.

The conditionally-averaged fluctuating flow field appears as if it were generated by two jets having opposite direction, strongly interacting in the VISA detection region and producing a complex flow behaviour.

The present observed scenario seems to be consistent with the conceptual model of coherent structure of Jeong et al. [16], already mentioned in the introduction. As sketched in *figure 9*, the flow structure obtained from the conditional analysis of the present DPIV data set may be speculatively interpreted as the flow field induced by two pre-existing adjacent overlapping counter-rotating vortices, asymmetrically tilted due to their mutual induction and advected by the mean flow. The organisation of the flow into low and high speed regions comes from the pumping of fluid away from and towards the wall respectively. According to the model, motions of opposite signs induced by the two counter-rotating vortices near the overlapping region would be responsible for the creation of the very strong internal shear layer detected here by the VISA technique.

In such a scenario, the asymmetric feature of the low speed streaks, recognised to be essential for the creation of strong shear layers, as also pointed out by Johansson et al. [8], would be related to the alternate tilting of the staggered vortices.

The complex vectorial phase-averaged flow field shown in *figure 7* gives evidence of the presence of strong spanwise u-velocity gradients ($\mathrm{d}u/\mathrm{d}z$) at the high speed-low speed interface, as it can be seen also in the single

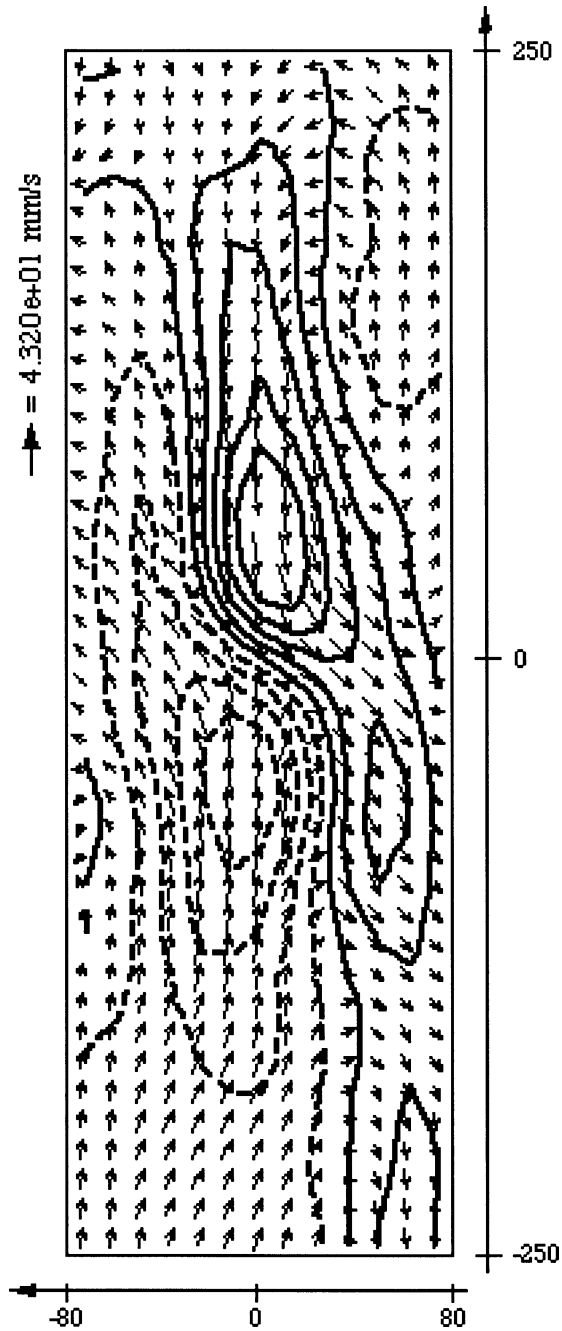

Figure 7. Conditional ensemble-averaged flow field ($y^+ = 20$). Contour lines: low-speed and high-speed streaks in mm/s; contours $= -32$, 32 increment 8. Vector plot: fluctuating velocity parallel to the wall.

realisations. This derivative constitutes the main contributor to the wall-normal vorticity, ω_y. In *figure 10* a grey-level map of VISA-event-conditioned wall-normal vorticity ω_y, superimposed on contour lines of low-speed and high-speed streaks of *figure 7*, is shown. The importance of the normal vorticity component in the turbulence production cycle has been, among others, stressed by Jimenez and Pinelli [38] and Schoppa and

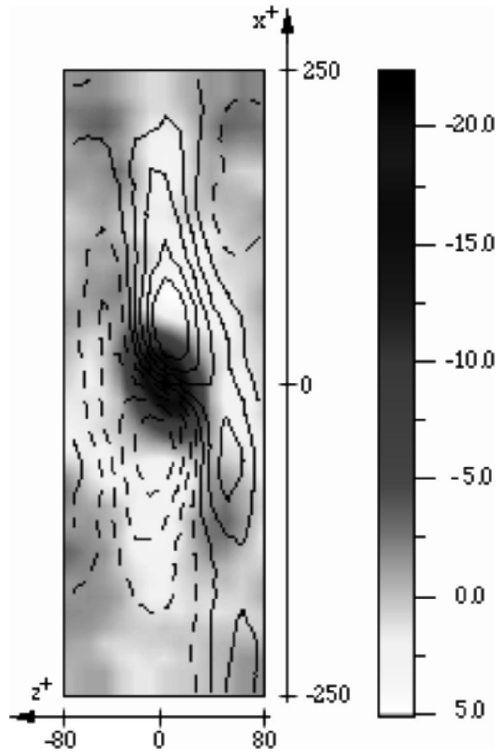

Figure 8. Conditional ensemble-averaged flow field ($y^+ = 20$). Contour lines: low-speed and high-speed streaks. Grey-level map: $\mathrm{d}u/\mathrm{d}x$ (s^{-1}).

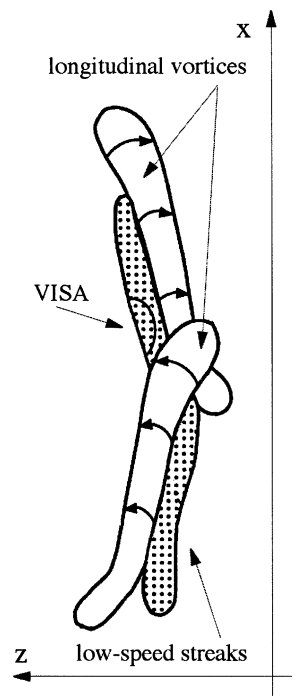

Figure 9. Quasi-longitudinal vortical structures and low-speed streaks (reference [16]).

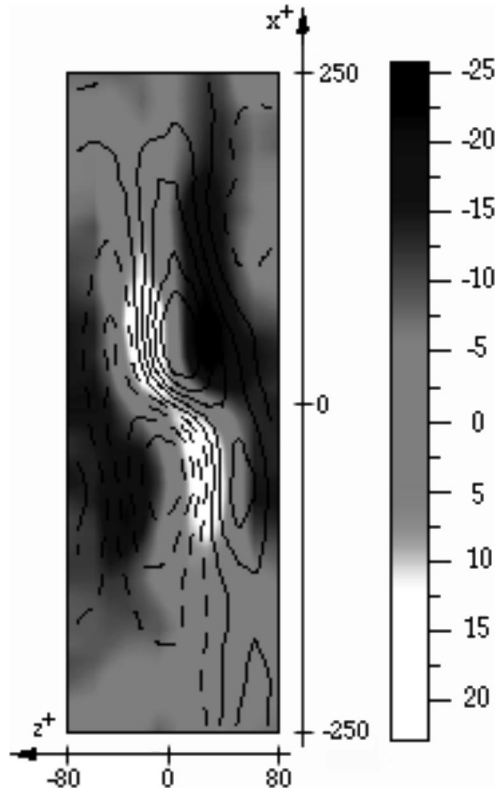

Figure 10. Conditional ensemble-averaged flow field ($y^+ = 20$). Contour lines: low-speed and high-speed streaks. Grey-level map: wall-normal vorticity ω_y (s^{-1}).

Hussain [19], according to whom the inviscid instability of the vorticity sheet (predominately $+\omega_y$) flanking the streak is the basic regeneration mechanism of streamwise vortices. Due to the lack of temporal resolution the present results do not allow any speculative consideration about the dynamic mechanisms leading to the streak instability growth, it is only possible to see from *figure 10* that the threshold value of ω_y postulated by schoppa and Hussain for the instability growth is exceeded in the region of the detected VISA event.

4. Concluding remarks

Results of measurements in the inner layer of a turbulent boundary layer on a flat plate have been shown.

A DPIV technique has been used to quantitatively investigate the flow in planes parallel to the wall, confirming that the technique is suitable for the study of wall turbulence.

The flow field in the buffer layer appears to be characterised by a streaky configuration, where elongated low-speed bands alternate with higher speed regions. The streamwise extent and spanwise spacing of the observed streaks are in agreement with previous investigations. Fourier analysis of the DPIV data permitted quantitative evaluation of the spanwise modes of the streaky structures; it has been found that the most energetic spanwise modes occur at $\lambda^+ = 260$ in the buffer layer and increase to $\lambda^+ = 370$ at $y^+ = 70$ and $\lambda^+ = 490$ at $y^+ = 130$.

Internal shear layer motions have been deduced using VISA technique and the detected events have been ensemble averaged centring individual realisations both in x and z directions. The spatial relationship between

low-speed streaks and internal shear layer motions has been inferred by the obtained ensemble averaged structure. The segmented and wavy nature of the low speed streaks has been recognised as strictly correlated to the existence of strong accelerated internal shear layers and then to the production of turbulent energy.

Strong values of ω_y, which are supposed to play an essential role in the turbulence regeneration cycle, have been captured on both sides of the streaks.

The average field is consistent with the scenario depicted by the most recent conceptual models for wall turbulence.

Acknowledgements

This research was funded by CSDF-CNR and by MURST grants.

References

[1] Kline S.J., Reynolds W.C., Schraub F.A., Runstadler P.W., The structure of turbulent boundary layers, J. Fluid Mech. 30 (1967) 741.
[2] Corino E.R., Brodkey R.S., A visual study of turbulent shear flow, J. Fluid Mech. 37 (1969) 1.
[3] Kim H.T., Kline S.J., Reynolds W.C., The production of turbulence near a smooth wall in a turbulent boundary layer, J. Fluid Mech. 50 (1971) 133.
[4] Blackwelder R.F., Haritodinis J.H., Scaling of the bursting frequency in turbulent boundary layers, J. Fluid Mech. 132 (1983) 87.
[5] Robinson S.K., Choerent motions in the turbulent boundary layer, Annu. Rev. Fluid Mech. 23 (1991) 601−639.
[6] Guezennec Y.G., Piomelli U., Kim J., On the shape and dynamics of wall structures in turbulent channel flow, Phys. Fluids A-Fluid 1 (4) (1989) 764.
[7] Kim J., Moin P., Moser R.D., Turbulence statistics in fully developed channel flow at low Reynolds number, J. Fluid Mech. 177 (1987) 133.
[8] Johansson A.V., Alfredsson P.H., Kim J., Evolution and dynamics of shear-layer structures in near-wall turbulence, J. Fluid Mech. 224 (1991) 579.
[9] Blackwelder R.F., Kaplan R.E., On the wall structure of turbulent boundary layer, J. Fluid Mech. 76 (1976) 89.
[10] Bernard P.S., Thomas J.M., Handler R.A., Vortex dynamics and production of Reynolds stress, J. Fluid Mech. 253 (1993) 385.
[11] Handler R.A., Hendricks E.W., Leighton R.I., Low Reynolds number calculation of turbulent channel flow: a general discussion, Naval Res. Lab. Mem. Rep. 6410, 1989.
[12] Brooke J.W., Hanratty T.J., Origin of turbulence-producing eddies in a channel flow, Phys. Fluids A-Fluid 5 (4) (1993) 1011.
[13] Chacin J.M., Cantwell B.J., Kline S.J., Study of turbulent boundary layer structure using the invariants of the velocity gradient tensor, Exp. Therm. Fluid Sci. 13 (1996) 308–317.
[14] Spalart P.R., Direct simulation of a turbulent boundary layer up to $R_\vartheta = 1410$, J. Fluid Mech. 187 (1988) 61.
[15] Theodorsen T., The structure of turbulence, in: Gortler, Tollmein (Eds), 50 Jahre Grenzschichtforsung, Vieweg and Sohn, Braunschweig, Germany, pp. 55–62.
[16] Jeong J., Hussain F., Schoppa W., Kim J., Coherent structures near the wall in a turbulent channel flow, J. Fluid Mech. 332 (1997) 185.
[17] Jeong J., Hussain F., On the identification of a vortex, J. Fluid Mech. 285 (1995) 69.
[18] Robinson S.K., The kinematics of turbulent boundary layer structure, NASA Tech. Mem. 103859 (1991).
[19] Jimenez J., On the structure and control of near wall turbulence, Phys. Fluids 6 (1994) 944.
[20] Schoppa W., Hussain F., Genesis and dynamics of coherent structures in near-wall turbulence: a new look, in: Panton R.L. (Ed.), Self Sustaining Mechanisms of Wall Turbulence, Computational Mech. Pubs., Southampton, 1997.
[21] Jimenez J., Pinelli A., The role of coherent structure interactions in the regeneration of wall turbulence, in: Frisch V. (Ed.), Advance in Turbulence, Kluwer Academic Publishers, 1998, p. 155.
[22] Gottero M., Onorato M., DPIV analysis of wall turbulent shear flows, in: 21st Congress of the International Council of the Aeronautical Sciences, Melbourne, Australia, 1998.
[23] Gottero M., Onorato M., DPIV investigation of near wall turbulent flow structures, in: 7th European Turbulence Conference, Saint Jean Cap Ferrat, France, 1998.
[24] Adrian R.J., Particle-imaging techniques for experimental fluid mechanics, Annu. Rev. Fluid Mech. 23 (1991) 261.
[25] Willert C.E., Gharib M., Digital particle image velocimetry, Exp. Fluids 4 (1991) 181.
[26] Westerweel J., Digital Particle Image Velocimetry. Theory and Application, Delft University Press, 1993.
[27] Kompenhans J., Hocker R., Investigation of turbulent flows by means of P.I.V., in: 5th Int. Symp. on Flow Vis., Prague, 1989.
[28] Eggels J.G.M., Unger F., Weiss M.H., Westerweel J., Adrian R.J., Friedrich R., Nieuwstadt F.T.M., Fully developed turbulent pipe flow: a comparison between direct numerical simulation and experiment, J. Fluid Mech. 268 (1994).

[29] Westerweel J., Draad A.A., van der Hoeven J.G.Th., van Oord J., Measurement of fully-developed turbulent pipe flow with digital particle image velocimetry, Exp. Fluids 20 (1996) 165.
[30] Fung J.C.H., Hunt J.C.R., Malik N.A., Perkins R.J., Kinematic simulation of homogeneous turbulence by unsteady random Fourier modes, J. Fluid Mech. 236 (1992) 281.
[31] Grotzbach G., Spatial resolution requirements for direct numerical simulation of the Rayleigh–Benard convection, J. Comput. Phys. 49 (1983).
[32] Antonia R.A., Teitel M., Kim J., Browne L.W.B., Low-Reynolds number-effects in a fully developed turbulent channel flow, J. Fluid Mech. 236 (1992) 579.
[33] Wei T., Willmarth W.W., Reynolds-number effects on the structure of a turbulent channel flow, J. Fluid Mech. 204 (1989) 57.
[34] Landahl M.T., On sublayer streaks, J. Fluid Mech. 212 (1990) 593.
[35] Smith C.R., Metzler S.P., The characteristics of low-speed streaks in the near-wall region of turbulent boundary layer, J. Fluid Mech. 129 (1983) 27.
[36] Liu Z.C., Adrian R.J., Hanratty T.J., A study of streaky structures in a turbulent channel flow with particle image velocimetry, in: Int. Symp. on the Application of Laser Technology to Fluid Mechanics, Lisbon, 1996.
[37] Kline S.J., in: Smith C.R., Abbot D.E. (Eds), Coherent Structure of Turbulent Boundary Layer, AFOSR/Lehigh University Workshop, Dept. Mech., Bethlehem, PA, 1978, p. 1.
[38] Jimenez J., Pinelli A., Wall turbulence: How it works and how to damp it, in: 28th AIAA Fluid Dynamics Conference, Snowmass Village, CO, 1997, Paper 97-2112.